






## Temporal Variability of Fluvial Sand Composition: An Annual Time Series From Four Rivers in SW Germany

L. Stutenbecker<sup>1</sup> , D. Scheuvsens<sup>2</sup>, M. Hinderer<sup>2</sup>, J. Hornung<sup>2</sup> , R. Petschick<sup>3</sup>, N. Raila<sup>2</sup> , and E. Schwind<sup>2</sup>

<sup>1</sup>Institute of Geology and Palaeontology, University of Münster, Münster, Germany, <sup>2</sup>Institute of Applied Geosciences, Technical University of Darmstadt, Darmstadt, Germany, <sup>3</sup>Institut für Geowissenschaften, Goethe University Frankfurt am Main, Frankfurt am Main, Germany

### Special Section:

Controls and Biasing Factors in Sediment Generation, Routing, and Provenance: Models, Methods, and Case Studies

### Key Points:

- Bed load sand from 4 rivers was sampled monthly over the course of 1 year to analyze the temporal compositional variability
- Composition is grain-size-dependent, and narrow grain-size fractions show less variability than bulk sediment samples
- Composition changes during the year, and this is related to changing grain-size distributions rather than changing sediment sources

### Correspondence to:

L. Stutenbecker,  
[lstutenb@uni-muenster.de](mailto:lstutenb@uni-muenster.de)

### Citation:

Stutenbecker, L., Scheuvsens, D., Hinderer, M., Hornung, J., Petschick, R., Raila, N., & Schwind, E. (2023). Temporal variability of fluvial sand composition: An annual time series from four rivers in SW Germany. *Journal of Geophysical Research: Earth Surface*, 128, e2023JF007138. <https://doi.org/10.1029/2023JF007138>

Received 1 MAR 2023

Accepted 5 JUN 2023

### Author Contributions:

**Conceptualization:** L. Stutenbecker

**Data curation:** L. Stutenbecker

**Formal analysis:** L. Stutenbecker, D. Scheuvsens, R. Petschick, N. Raila, E. Schwind

**Investigation:** L. Stutenbecker, D. Scheuvsens

**Methodology:** L. Stutenbecker, D. Scheuvsens

**Project Administration:** L. Stutenbecker

© 2023. The Authors.

This is an open access article under the terms of the [Creative Commons Attribution License](https://creativecommons.org/licenses/by/4.0/), which permits use, distribution and reproduction in any medium, provided the original work is properly cited.

**Abstract** The sampling of fluvial sediment is subject to many sources of uncertainty, for example, time and location, and the number of samples collected. It is nevertheless commonly assumed that a sample taken at one time and location provides a somewhat averaged compositional signal. Any spatial or temporal variability of this signal is often neglected. This study investigates how the composition of bed load sand changes over an observation period of 1 year in four river basins with differing bedrock geology in southwestern Germany. Up to 12 bulk sediment samples were taken at the same locations using the same approach and analyzed for their granulometry and geochemistry. The results indicate that (a) different grain sizes yield different compositions due to source rock composition and hydraulic sorting effects, (b) bulk sediment composition changes temporally due to changing grain-size distribution, and (c) compared to the bulk sample, the composition of narrow grain sizes is temporally more stable but nevertheless has an average variability of 15%. Because heavy mineral-bound elements such as Zr have the highest variability, we relate a major component of compositional variability to temporally varying heavy mineral concentrations in response to hydrodynamic processes. Mixing modeling demonstrates that the fluvial sand faithfully reflects its catchment geology and that the sediment sources do not change substantially during the observation period, even during a flooding event. We conclude (a) that the causes for compositional variability may be disentangled using chemical and granulometric time series data and (b) that narrow grain sizes yield representative source rock contributions.

**Plain Language Summary** Sediment transported by rivers is generated by the erosion of the rocks present within the river catchment area. The composition of this sediment is controlled by various processes in the catchment, for example, climate, rock type, weathering, and flow strength. Geoscientists can use modern river sediment to understand how these processes impact sediment composition, and then apply this information to the geologic time. Sampling the river sediment is often the first step in such studies, but few studies consider the sources of uncertainty during sampling, for example, time and location of sampling, and number of collected samples. For this study, we returned to the same river location during the course of 1 year to take bulk sediment samples and analyzed how variable the size of sediment grains and the sediment chemistry are. We discovered that different grain sizes yield different chemical compositions, and this is caused by differences in rock type and hydraulic processes. Because the proportion of different grain sizes in the bulk sediment changes over the year due to water flow conditions, the chemistry of the bulk sediment sample changes over the year. We provide some quantitative estimates for this variability that should be considered in similar studies.

## 1. Introduction

Fluvial sediment and sedimentary rock contain diverse information that is encrypted in their sedimentary structures, grain-size distributions, grain shapes, chemical compositions, isotope ratios, or mineral contents. Deciphering this information can increase our knowledge of the past and present geological, climatic, or hydrological processes acting in the source area or in transit. For instance, just a bucket or a handful of sediment is considered enough to calculate catchment-wide denudation rates from cosmogenic nuclide ratios (e.g., von Blanckenburg, 2005) to determine sediment sources through provenance analysis (e.g., Garzanti et al., 2007), or to infer hydraulic information from grain-size distributions (e.g., Litty et al., 2016).

**Resources:** L. Stutenbecker, D. Scheuven, M. Hinderer, J. Hornung  
**Supervision:** L. Stutenbecker  
**Validation:** L. Stutenbecker  
**Visualization:** L. Stutenbecker  
**Writing – original draft:** L. Stutenbecker  
**Writing – review & editing:** L. Stutenbecker, D. Scheuven, M. Hinderer, R. Petschick, N. Raila, E. Schwind

Infrequent short-term sediment transport events such as debris flows or major floods and their corresponding deposits continue to receive increasing attention and may be successfully distinguished from typical “background” deposition (Berger et al., 2011; Schillereff et al., 2014). In this context, many studies have focused on the positive correlation between water discharge and suspended sediment concentration (e.g., Cohen et al., 2014; Rousseau et al., 2019; van der Perk & Espinoza Vilches, 2020; Walling & Moorehead, 1987; Xu, 2002). Some studies have analyzed the short-term variability of suspended sediment composition and linked this to changes in sediment source contributions, for example, by the seasonal (de)activation of glacial sources (Amann et al., 2022; Stutenbecker et al., 2019), storm and flood events (Douglas et al., 2008; Liu et al., 2022; Navrátil et al., 2012), hydraulic conditions (Bouchez et al., 2011; Rousseau et al., 2019; van der Perk & Espinoza Vilches, 2020), and anthropogenic processes such as sediment abstraction, artificial sediment trapping, pollution, and agriculture-induced soil erosion (Carter et al., 2006; Florsheim et al., 2011; Lane et al., 2019; Navrátil et al., 2008).

However, many methods still rely on the assumption that a sediment sample taken at one time at one location in a river exhibits a somewhat averaged composition that reflects typical erosion and transport processes (“let nature do the averaging” principle, von Blanckenburg, 2005). Short-term chemical or mineralogical variability seems to be considered negligible in this context. It appears to be a common consensus that large catchments with complex internal feedbacks and potentially long sediment residence times average out short-term compositional variability (Romans et al., 2016), whereas small catchments may not be dynamic enough to produce substantial variability in the first place. Consequently, reported sediment mineralogy and chemistry are limited to a few samples or even only one measurement in many rivers (Müller et al., 2021). Complete time series are very rare and limited to suspended sediment (Rousseau et al., 2019; van der Perk & Espinoza Vilches, 2020), which tends to be dominated by silt and clay (Stone & Saunderson, 1992; Walling & Moorehead, 1987; Walling & Woodward, 2000; Xu, 2002). However, many geological methods such as provenance and cosmogenic nuclide analysis target the sand-sized sediment transported as bed load (e.g., Garzanti et al., 2009; Ingersoll et al., 1984; van Dongen et al., 2019), for which the short-term compositional variability remains poorly documented.

This study aims to test how bedload sediment composition changes at an annual scale using the case study of four rivers located in southern Germany with different bedrock lithologies. We hypothesize that (a) the bulk sediment composition changes mostly due to variations in grain-size distribution, which in turn might be controlled by hydraulic conditions such as water discharge (Walling & Moorehead, 1987; Xu, 2002) and (b) the composition of narrow grain-size fractions should stay constant if the sediment sources stay constant. Accordingly, we collected one bulk sediment sample per month over the period of 1 year at the same location and analyzed the chemical composition of the sediment in six narrow grain-size windows (2–1, 1–0.5, 0.5–0.25, 0.25–0.125, 0.125–0.063, and <0.063 mm). Using granulometric, geochemical, and mineralogical information, as well as a linear multivariate mixing model, we analyze the impact of source rock composition and texture, weathering, and hydraulic sorting on sediment composition.

## 2. Setting

The Gersprenz, Modau, Mümling, and upper Neckar rivers drain lithologically heterogeneous catchments of different sizes (90–2,000 km<sup>2</sup>, Table 1) in southwestern Germany (Figure 1). They are overall characterized by moderate relief, high vegetation cover, and a temperate climate (Table 1).

The Gersprenz, Modau, and Mümling rivers are located in the Odenwald, an eastern rift shoulder of the Upper Rhine Graben, which forms a segment of the European Cenozoic rift system (Ziegler, 1992). The Odenwald rift shoulder was uplifted during the Neogene and Quaternary (Peters & van Balen, 2007) and contains remnants of a Paleozoic magmatic arc formed during the Variscan orogeny as well as its Permo-Triassic sedimentary cover (Stein, 2001). The Gersprenz and Modau catchments are underlain by Paleozoic granitoid, diorite, quartz diorite, gabbro, amphibolite, orthogneiss, and minor meta-sedimentary rocks (paragneiss, schist). In contrast, the Mümling catchment drains predominantly Permian to Triassic siliciclastic sandstone and mudstone with minor intercalated Permian dolomite (Figure 1a). In addition, loess and eolian sand occur in all three catchments. The eolian sediment was mobilized and blown out from the Rhine river plain and deposited on the hillslopes of the Odenwald during the Pleistocene (Pflanz et al., 2022).

The upper Neckar river drains the hilly terrain of the South German Scarplands, formed during the Paleogene and Neogene as a result of the Rhine graben rifting and successive southeastward migration of escarpments.

**Table 1**  
Basic Information About the Four Sampling Sites

	Gersprenz	Modau	Mümling	Upper Neckar
Sampling location	49°51'40.2"N 8°50'44.7"E	49°49'09.4"N 8°39'41.4"E	49°50'36.0"N 9°05'36.0"E	48°30'02.5"N 9°01'16.5"E
Catchment area at sampling point (km <sup>2</sup> ) <sup>a</sup>	290	90	360	2,000
Relief (m) <sup>b</sup>	468	481	448	701
Mean water discharge (m <sup>3</sup> /s) <sup>c</sup>	2.98	0.68	3.24	14.54
Mean annual rainfall (mm) <sup>d</sup>	921	915	938	953
Mean annual surface temperature (°C) <sup>e</sup>	9.51	9.4	9.1	7.87
Land cover <sup>f</sup>	35	38	60	38
Forest (%)	33	31	24	28
Low vegetation (%)	22	17	10	21
Agriculture (%)	7	10	5	10
Built-up land (%)	3	4	1	3
Bare soil (%)	50	34	6	0
Bedrock geology <sup>g</sup>	11	32	0	0
Granitoid/gneiss/schist (%)	5	1	80	25
Diorite/gabbro/amphibolite (%)	1	0	1	49
Clastic sedimentary rock (%)	33	33	13	26
Carbonate rock (%)				
Quaternary cover (%)				

<sup>a</sup>Catchment areas were calculated in ArcGIS from the sampling spot upstream using the SRTM 1 arc-second (~30 m) digital elevation model, available via <https://earthexplorer.usgs.gov/>. <sup>b</sup>Relief was calculated in ArcGIS as the difference between the maximum and minimum elevation in each catchment using the SRTM 1 arc-second (~30 m) digital elevation model, available via <https://earthexplorer.usgs.gov/>. <sup>c</sup>Water discharge is given as the average from daily discharge measurements over the 1-year-observation period (April 2019–March 2020 and January 2020–December 2020, respectively). The data for the gauging stations Harreshausen (Gersprenz river), Eberstadt (Modau river), and Hainstadt (Mümling river) is provided by the Hessisches Landesamt für Naturschutz, Umwelt und Geologie, Wiesbaden, the data from the gauging station Horb (Neckar river) by the Landesanstalt für Umwelt Baden-Württemberg. <sup>d</sup>Rainfall data were extracted as mean values for each catchment from gridded 1950–2021 E-OBS data (Cornes et al., 2018), data available via [https://surfobs.climate.copernicus.eu/dataaccess/access\\_eobs.php#datafiles](https://surfobs.climate.copernicus.eu/dataaccess/access_eobs.php#datafiles). <sup>e</sup>Surface temperature data were extracted as mean values for each catchment from gridded 1950–2021 E-OBS data (Cornes et al., 2018), data available via [https://surfobs.climate.copernicus.eu/dataaccess/access\\_eobs.php#datafiles](https://surfobs.climate.copernicus.eu/dataaccess/access_eobs.php#datafiles). <sup>f</sup>Land cover from 2020 Sentinel-2 data (Riembauer et al., 2021), data available via [https://data.mundialis.de/geodata/luc-germany/classification\\_2020/classification\\_map\\_germany\\_2020\\_v02.tif](https://data.mundialis.de/geodata/luc-germany/classification_2020/classification_map_germany_2020_v02.tif). <sup>g</sup>Bedrock geology is given as the area percentage of main bedrock lithologies present in each catchment, extracted from 1:200,000 geological maps provided by Federal Institute for Geosciences and Natural Resources, Germany (2007).

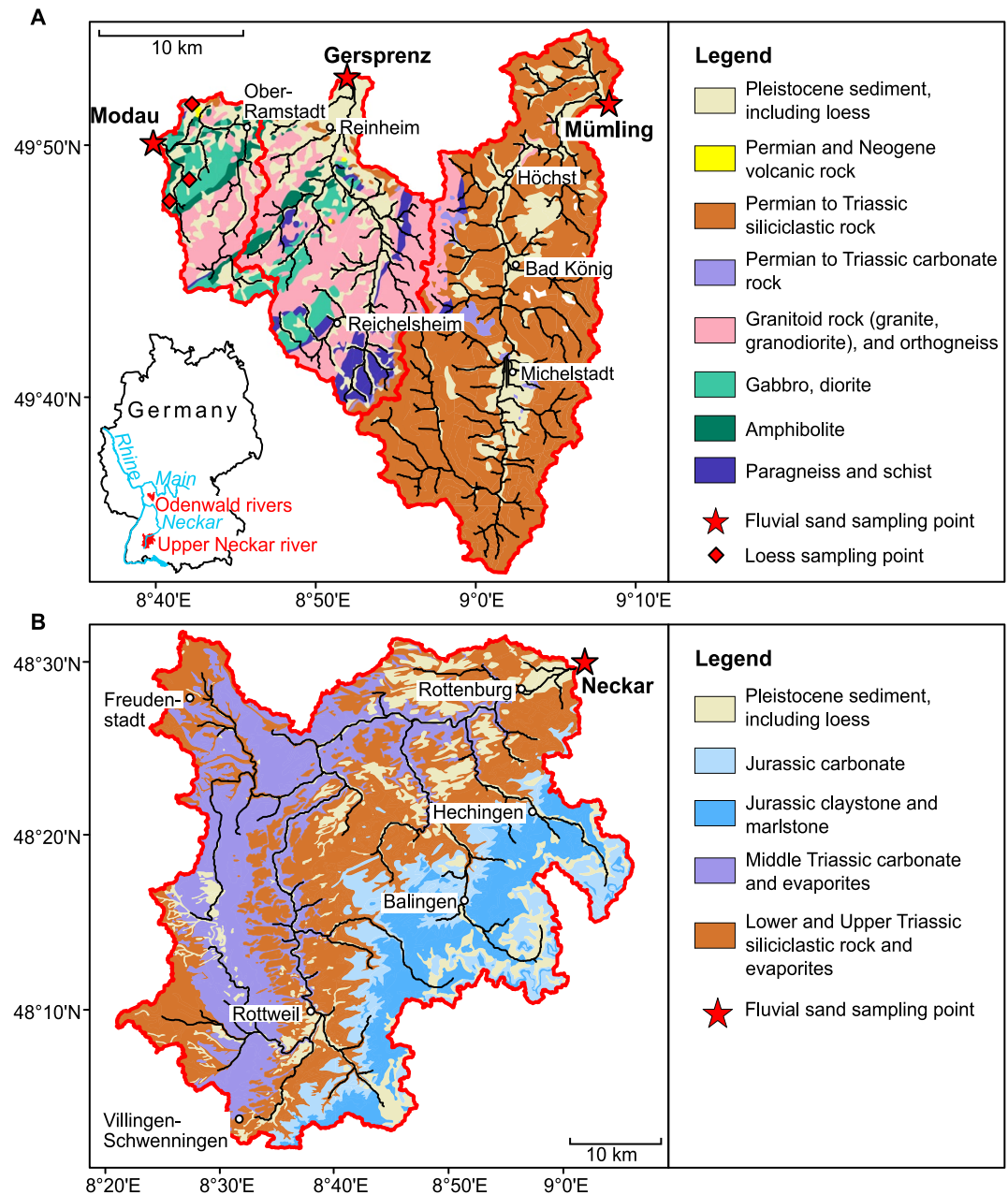


**Figure 1.** Setting, geology, catchment outlines, and river network of the studied river basins. (a) The three Odenwald rivers Modau, Gersprenz, and Mümling. (b) The upper Neckar basin. Geology according to the 1:200,000 geological maps of the Federal Institute for Geosciences and Natural Resources, Germany (2007), sheets CC 6318 (Frankfurt am Main-Ost), CC 7918 (Stuttgart-Süd), and CC 7910 (Freiburg-Nord).

It comprises siliciclastic and carbonate rocks (Figure 1b) deposited during the Triassic and Jurassic in the Central European Basin, a Pangean intracontinental basin formed in the aftermath of the Variscan orogeny (Littke et al., 2008). Specifically, these are Early Triassic terrestrial sandstone (Buntsandstein Group), Middle Triassic marine carbonates (Muschelkalk Group; mostly limestone, marlstone, and dolostone, additionally some evaporites), Late Triassic mixed lacustrine, fluvial and shallow marine siliciclastic rocks (Keuper Group; sandstone, siltstone, claystone, evaporites), and Jurassic carbonates (limestone, intercalated with claystone and marlstone). Quaternary deposits include widespread Pleistocene loess and Pleistocene to Holocene fluvial sediment.

### 3. Materials and Methods

#### 3.1. Sampling and Sample Preparation

In total, 46 sediment samples were collected in 2019 and 2020; 12 sediment samples from the Gersprenz river between January 2020 and December 2020, 10 samples from the Modau river between May 2019 and April 2020, 12 samples from the Mümling river between January 2020 and December 2020, and 12 samples from the Neckar river between April 2019 and March 2020. The samples were collected on unvegetated parts of lateral bars with active erosion and deposition of mostly sand-sized sediment. Samples were taken by the same operator by scooping the uppermost 1–2 cm of sediment from the sand bar surface over an area of approximately 1 m<sup>2</sup> until 0.5–2 kg of sediment was obtained. Using trees on the shore and boulders in the river as orientation, we estimate our location accuracy to be within 1 m<sup>2</sup>.

The hydraulic conditions were monitored during the sampling period using water level and discharge data from nearby gauging stations operated by the responsible regional environmental agencies (Table 1). To test the potential contribution of loess deposits, we took three additional samples of loess and eolian sand from the western Modau catchment (Figure 1).

The sediment was oven-dried at 105°C and sieved to <2 mm to remove the pebble fraction as well as occasional plant debris. From the <2 mm fraction, one part of the sample was separated using a riffle splitter and reserved for later analysis to characterize the bulk composition. The remaining <2 mm sample was wet-sieved to the following six grain-size fractions: 2–1 mm (–1–0 Φ), 1–0.5 mm (0–1 Φ), 0.5–0.25 mm (1–2 Φ), 0.25–0.125 mm (2–3 Φ), 0.125–0.063 mm (3–4 Φ), and <0.063 mm (>4 Φ). The silt and clay fractions (>4 Φ) were carefully obtained by loss-free settling. The sieved fractions were dried at 105°C and weighed.

#### 3.2. XRF and XRD Analysis

Of the 46 samples with 7 sub-samples each (bulk sample and the six individual grain-size fractions), 172 sub-samples with enough material (>10 g) were further processed for major element geochemical analysis. The samples were ground in tungsten carbide vessels using a Siebtechnik vibrating disc-mill TS. The powder was mixed with a binding agent (Hoechst Wax C) with a mixing ratio of 4:1, homogenized in a rotator, and pressed into pellets in Alu cups. The chemical analysis of the pressed powder pellets was performed with the wavelength-dispersive X-ray spectrometer S8 Tiger 4 kW (Bruker) at the Technical University of Darmstadt, which is equipped with a Rhodium X-ray tube. For the analysis of the elemental concentrations, the “standard-less” evaluation method Quant Express Best Detection was used (qebd 34 mm-vac). Quant Express Best Detection was calibrated by Bruker with numerous diverse standards and is checked on a monthly basis at the Technical University of Darmstadt with different reference standards. The major element oxides SiO<sub>2</sub>, TiO<sub>2</sub>, Al<sub>2</sub>O<sub>3</sub>, Fe<sub>2</sub>O<sub>3</sub>, MnO, MgO, CaO, Na<sub>2</sub>O, K<sub>2</sub>O, and P<sub>2</sub>O<sub>5</sub>, as well as the trace elements Zn, Rb, Sr, Zr, and Ba, were measured. All analyses were normalized to 100 wt. %. Loss of ignition was not determined.

Due to temporal and financial constraints, only one sample per river was analyzed further using X-ray diffraction (April 2020 for the Gersprenz, February 2020 for the Modau, May 2020 for the Mümling, and November 2019 for the Neckar). The measurements were made by a Panalytical X'Pert Pro diffractometer at the Goethe University Frankfurt using a Copper anode (40 KV, 30 mA), automatic divergence slit, spinning of the sample holder, and Ni Filter to reduce K<sub>β</sub> and scatter radiation. Detection was performed using a Panalytical X'Celerator with multiple stripe characteristics. About 1–2 g of powdered samples were prepared by backside filling into steel sample holders to reduce the texturation of non-isotropic mineral phases. Each powder was measured between 2.5° and 70°2θ. Phase validations were supported by *Powder Diffraction File 4 Minerals* of the *International Centre of Diffraction Data*. For semiquantitative phase calculation, the intensities of characteristic lines of each detected mineral were calculated to a fixed divergence condition and weighted after conversion using standardized *Reference Intensity Ratios*. The following *Reference Intensity Ratio* factors have been used: quartz: 3.03; alkali feldspar: 0.6; plagioclase: 0.68; calcite: 3.2; dolomite: 2.51; amphibole (hornblende): 0.73; illite/muscovite: 0.43; kaolinite and chlorite: 1.0; goethite: 2.79; hematite: 3.26. In the case of clay minerals, only approximated results are available due to their small and broad Bragg reflexes and as a result of using only non-oriented bulk samples.

The Pearson correlation coefficient was calculated to check the correlation between mineral and element pairs as well as between geochemistry and mineralogy. Correlations with *p*-values < 0.05 are considered statistically significant.



### 3.3. Source Rock Database, Mixing Modeling, and Weathering Indices

The relationship between the source rocks and the fluvial sediment is complicated by many factors, including weathering intensity, lithology, transport, and depositional processes (Caracciolo, 2020; von Eynatten et al., 2012, 2016). To properly interpret the sediment composition, we compared geochemical data from various source rocks in the area from the literature with the river sand. We compiled 81 geochemical analyses from potential source rocks from the Odenwald area (Altenberger et al., 1990; Altherr et al., 1999; Poller et al., 2001; Reischmann et al., 2001; Siebel et al., 2012; Soyk, 2015; Will & Schmädicke, 2001; Will et al., 2015, 2021). Unfortunately, source rock data from the Neckar catchment were virtually not available in the literature, and own geochemistry data from the area are limited to Keuper sandstone, which only covers a quarter of the catchment area. For this reason, our analysis will focus mostly on the three rivers and the source rocks in the Odenwald.

In order to quantify the source rock contribution to the sediment and to identify potential source changes through time, we used a linear multivariate mixing model (Collins et al., 1996; Weltje, 1997). In the first step, principal component analysis based on log-ratio transformed geochemical data was used on the compiled source rock data to identify statistically distinguishable source classes. These classes were then used as input into the mixing model “fingerPro” in the R environment (Lizaga et al., 2020; R Core Team, 2021). Only major oxides were used because the compiled literature data rarely report trace-element compositions. This linear multivariate mixing model predicts the relative contribution of the considered source categories by finding the best fit between observed and calculated sediment composition. We used the in-built linear discriminant analysis, the range, and the Kruskal-Wallis-H-test to select the best combination of fingerprinting proxies and ran the model with 10,000 iterations.

The role of chemical weathering in the transformation from source rock to sediment is often assessed using geochemistry-based weathering indices (Buggle et al., 2011; Garzanti & Resentini, 2016; Hatano et al., 2019). Most weathering indices essentially measure the leaching of the mobile elements Ca, Na, and K relative to immobile Al during feldspar weathering (Buggle et al., 2011; Nesbitt & Young, 1982). In this context, Ca contents are used with the assumption that all CaO is silicate-bound and not carbonate-bound. Since carbonate rock is common in the Neckar catchment, this assumption is not justified in our study area and we chose to use the modified chemical index of alteration CIX of Garzanti et al. (2014), which excludes Ca and is calculated as  $CIX = Al_2O_3 / (Al_2O_3 + Na_2O + K_2O) * 100$ . We calculated the CIX for the river sediment and the source rock compiled from the literature.

## 4. Results

### 4.1. Hydrologic Condition and Grain-Size Distribution

During the observation period, the water level and discharge data of the responsible environmental agencies show their highest values during February and March 2020 and their lowest values in the summer months for all four rivers (Figure 2b). The four investigated rivers show different degrees of variation in their grain-size distributions (Figure 2a). The strongest grain-size variability is observed in the Gersprenz river where during December 2019 and February 2020 predominantly muddy sediment was deposited, and medium- to very coarse-grained sand during the rest of the year. The field observations and the hydrological data reveal that the mud derives from the deposition of suspended sediment at high water discharge and water levels and flooding of the sampled sand bar. The sampling location in the Modau river had high amounts of medium-grained to coarse-grained sand from June–August 2019 and February–April 2020, whereas from September 2019 to January 2020 more mud as well as very fine- and fine-grained sand were deposited. The Mümling river deposited similar amounts of mud and very fine-grained sand throughout the year, while the medium- to fine-grained sand ratio varied. Specifically, during January–February, June–August, and November–December, more medium-grained sand was deposited at the cost of fine-grained sand. The sampling spot is virtually lacking any sand coarser than  $2 \Phi$ . Different to the other three locations, the Neckar river sampling site included the coarsest-grained material with abundant pebbles. The amount of very coarse-grained sand increased from July 2019 to January 2020. The amount of mud at the sampling site was always <5%.

### 4.2. Geochemistry

The four river sediments differ substantially in their bulk geochemical composition (Figure 3a). The Modau and Gersprenz river sand has a relatively similar composition with around 70%  $SiO_2$  and 10%  $Al_2O_3$ , but the Modau

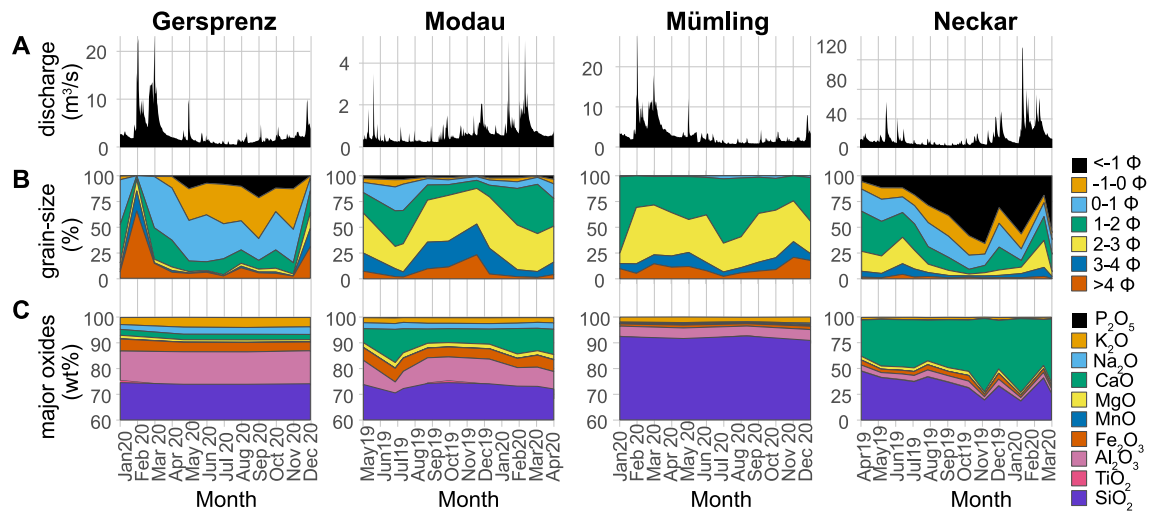


**Figure 2.** Annual variability of water discharge ((a); note different y-axis ranges), bulk sediment grain size ((b); in weight percentage of  $\Phi$  units), and major element sediment geochemistry (c). Panel (a) is compiled from Hessian Agency for Nature Conservation, Environment and Geology (2020) and Landesanstalt für Umwelt Baden-Württemberg (2020). Note that for panel (c) we display only the major element oxides. The y-axis of the  $\text{SiO}_2$ -dominated rivers Gersprenz, Modau, and Mümling is cut off at 60 wt. % to better display the variability of the element oxides with lower concentrations.

sand has higher CaO contents (8% average in the bulk sediment vs. 2% in the Gersprenz). The Mümling river sand is composed of almost 90%  $\text{SiO}_2$ , whereas the Neckar river sand has the highest CaO concentrations (up to 50%).

For most elements and element oxides, there is substantial variability within the different sub-fractions of each sample (“intra-sample variability,” Figure 4).  $\text{TiO}_2$ ,  $\text{Fe}_2\text{O}_3$ ,  $\text{P}_2\text{O}_5$ , Zn, and Zr increase with decreasing grain size

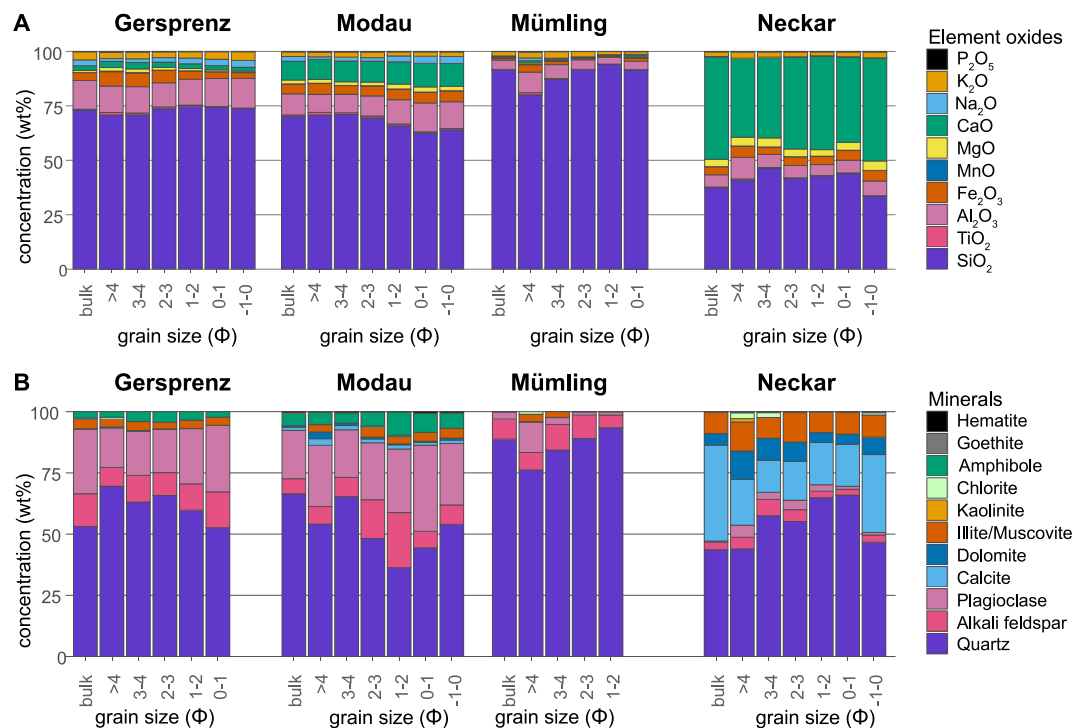


**Figure 3.** Average major element oxide (a) and mineralogical (b) composition of sediment from the four rivers. Note that the XRF results are calculated mean concentrations from all 46 samples, whereas XRD analysis was performed only on one sample per river (April 2020 for the Gersprenz, February 2020 for the Modau, May 2020 for the Mümling, and November 2019 for the Neckar).

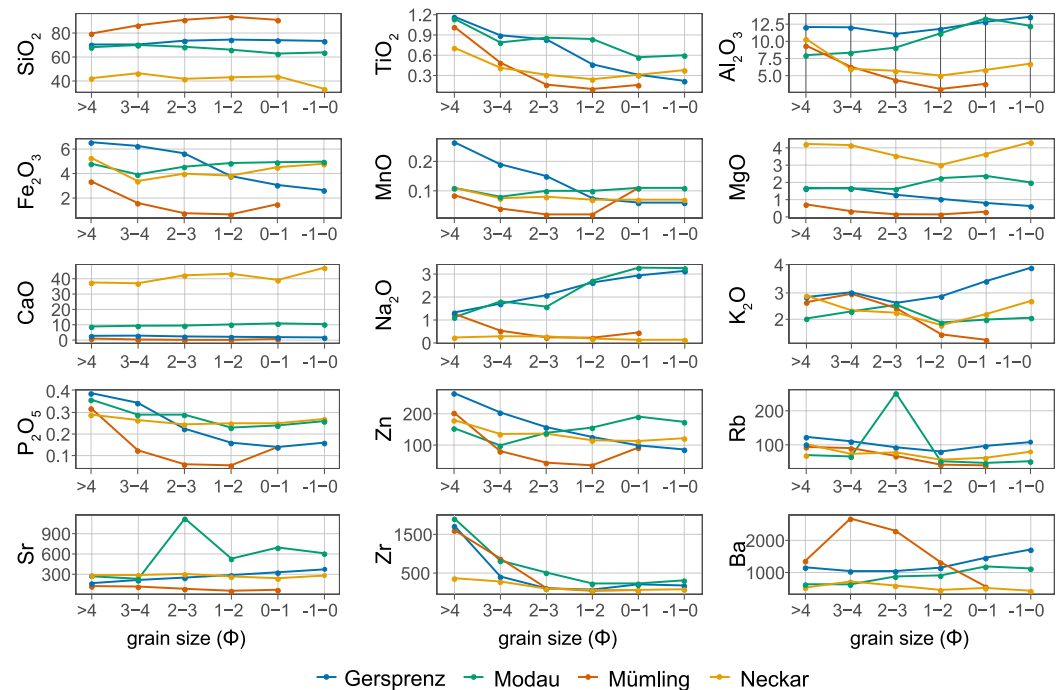


**Figure 4.** Median variability of sediment geochemistry for the different grain-size fractions. Y-axes are in wt. % for oxides and in ppm for trace elements.

in all four rivers.  $\text{Al}_2\text{O}_3$  and  $\text{Na}_2\text{O}$  show grain-size-dependent trends in some rivers but not in others. For example, their concentrations decrease with decreasing grain size in the Modau and Gersprenz, but have the opposite trend in the Mümling and Neckar.  $\text{K}_2\text{O}$  increases with decreasing grain size in the Mümling river and has the opposite trend in the Gersprenz river.  $\text{MnO}$  is highest in all  $>4 \Phi$  fractions but does not have a consistent trend in the sand fraction. Other oxides and elements ( $\text{SiO}_2$ ,  $\text{MgO}$ ,  $\text{CaO}$ ,  $\text{Sr}$ ,  $\text{Ba}$ , and  $\text{Rb}$ ) do not have any clear grain-size-dependent trend in any of the studied river samples.

The temporal chemical variability, expressed as relative standard deviation per grain-size class is on average around 18%, but is considerably higher for  $\text{Zr}$ ,  $\text{Ba}$ ,  $\text{Zn}$ ,  $\text{MnO}$ ,  $\text{P}_2\text{O}_5$ , and  $\text{TiO}_2$  (Figure 5). In general, the bulk samples and the fraction  $>4 \Phi$  have the highest relative standard deviation with average values around 20%–25%. The other (narrower) sand fractions have overall smaller relative standard deviations, but still in the order of around 15%. The Modau and Neckar rivers have the overall largest variability (average 22%), followed by the Mümling (average 17%) and the Gersprenz (average 12%).

The mean analytical error for all 172 samples and the 15 oxides and elements considered here is 2%. Individual analyses yielded uncertainties for  $\text{Zr}$  and  $\text{Ba}$  higher than 10%, but all other elements always have uncertainties  $<10\%$ . The mean analytical error for the main oxides is generally  $<3\%$  (except  $\text{P}_2\text{O}_5$ , mean 4%), and between 1% and 6% for the trace elements  $\text{Zn}$ ,  $\text{Rb}$ ,  $\text{Sr}$ ,  $\text{Zr}$ , and  $\text{Ba}$ , that is, the intersample and intrasample variability is about one order of magnitude higher than the analytical uncertainty.

The principal component analysis demonstrates that the samples from the four rivers are geochemically distinct (Figure 6). Also, a distinct grain-size trend is present for all four rivers, with fine-grained fractions plotting closer to the origin of the biplot than the coarse-grained fractions. When also using the five measured trace elements ( $\text{Zn}$ ,  $\text{Rb}$ ,  $\text{Sr}$ ,  $\text{Zr}$ , and  $\text{Ba}$ ) as input into the principal component analysis, the discrimination between the four rivers becomes less clear, mostly due to the high  $\text{Zr}$  concentration in the  $>4 \Phi$  fraction and high loading of  $\text{Zr}$ .

The CIX values range between 61 and 77 and vary between the samples, with the highest values observed in the  $>4 \Phi$  fraction (Figure 7a). The Neckar and Modau samples show overall the highest CIX values (median 71.4 and 71.2, respectively), followed by the Gersprenz samples with a median CIX of 68.3, and the Mümling samples with a median CIX of 64.5 (Figure 7b).



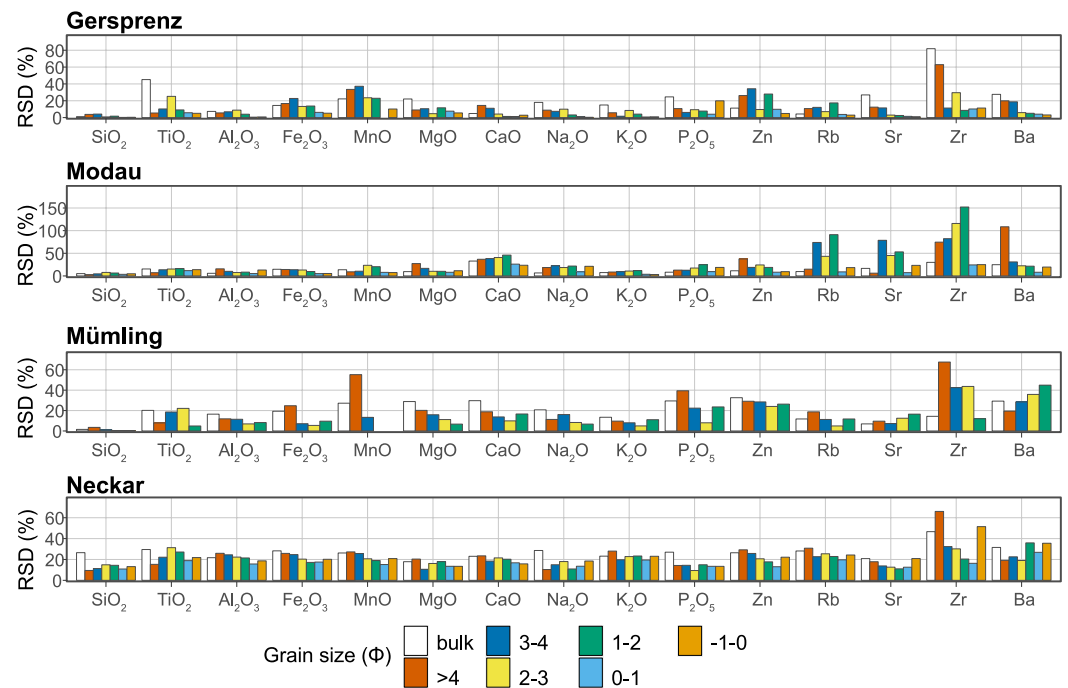


**Figure 5.** Temporal variability of all elements and element oxides, expressed as relative standard deviation (in %) per grain-size class.

### 4.3. Mineralogy

On average, the Gersprenz river sand is composed of 61% quartz, 11% alkali feldspar, 21% plagioclase, 3% amphibole, and 3% illite/muscovite (Figure 3b). The bulk Modau river sand has a relatively similar composition with 53% quartz, 11% alkali feldspar, 25% plagioclase, 6% amphibole, and 3% illite/muscovite, but with additional carbonate content of 2% calcite and 1% dolomite.

The Mümling river sand contains on average 86% quartz, 8% alkali feldspar, 4% plagioclase, and 1% illite/muscovite. The Neckar river sand has the highest carbonate content with an average of 29% calcite and 7% dolomite,

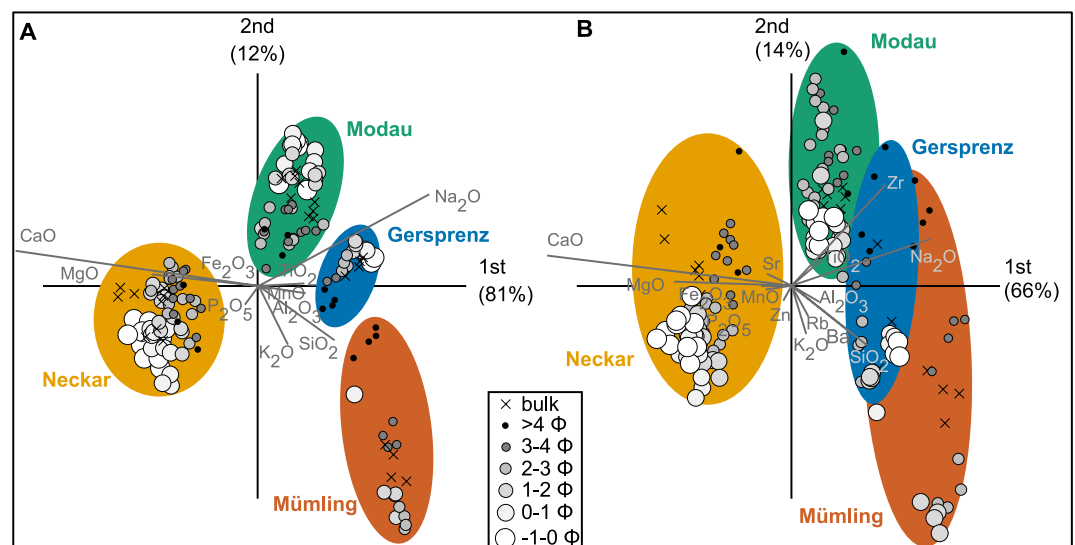


**Figure 6.** Results from principal component analysis using log-ratio transformed data as input. (a) Major element oxides only. (b) major element oxides and the five measured trace elements.

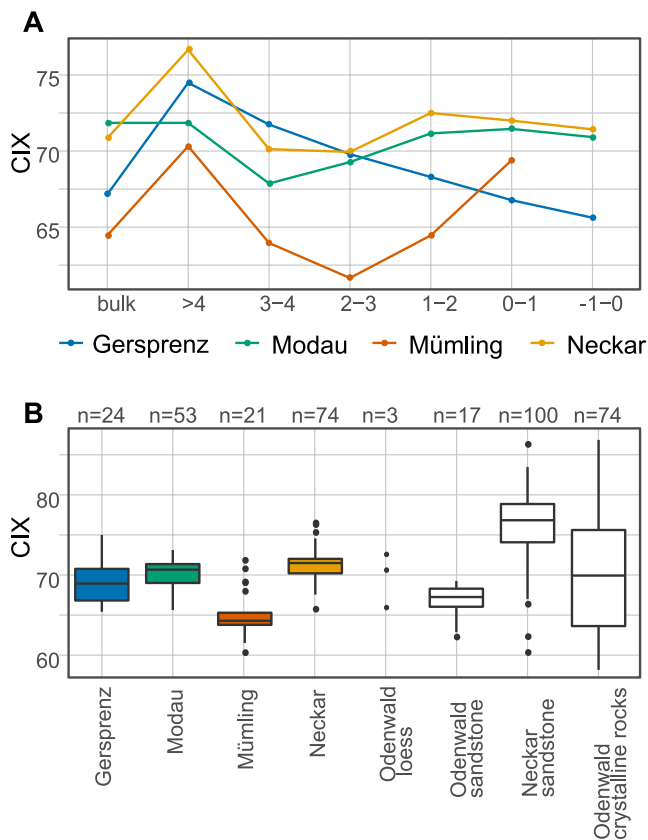


**Figure 7.** (a) Median CIX values of all grain-size fractions of each river. (b) Box-and-whisker-plots (boxes with 25th, 50th [median] and 75th percentile of CIX values) for the river sediment samples and compiled source rocks from the Odenwald sandstone (Early Triassic Buntsandstein Group, Soyk, 2015), Neckar sandstone (Late Triassic Keuper sandstone, unpublished data from drillings in the Neckar catchment), Odenwald loess (unpublished data, this study), and Odenwald crystalline rocks (Altenberger & Besch, 1993; Altenberger et al., 1990; Altherr et al., 1999; Poller et al., 2001; Reischmann et al., 2001; Siebel et al., 2012; Will & Schmädicke, 2001; Will et al., 2015, 2021).

and additionally 47% quartz, 4% alkali feldspar, 2% plagioclase, 9% illite/muscovite, and 1% chlorite.

Grain-size-dependent intra-sample mineralogical trends are less pronounced than in the chemical data (Figure 8). There is no general trend for any of the minerals that are common to all four river sediments. In the Mümling and Neckar river sands, alkali feldspar and plagioclase contents increase with decreasing grain size. In the Gersprenz sediment, alkali feldspar contents are higher in the coarse-grained fractions than in the fine-grained fractions. In the Modau sediment, plagioclase contents are higher in the coarse-grained than in the fine-grained sediment, but alkali feldspar contents are highest in the mid-sized sand fractions. The quartz content decreases with decreasing grain size in the Mümling river, but not in the other three rivers. Where present, kaolinite, chlorite, and dolomite increase with decreasing grain size. Amphibole, illite/muscovite, calcite, hematite, and goethite have no clear grain-size trend.

A strong positive correlation between mineralogy and chemistry (Figure 9) hints toward mineral chemistry but also toward the co-existence (and therefore provenance) of certain minerals. High feldspar contents are accompanied by high  $\text{Al}_2\text{O}_3$ ,  $\text{Na}_2\text{O}$ ,  $\text{K}_2\text{O}$ , Rb, and Ba concentrations. High calcite and dolomite contents are manifested by high CaO and MgO contents. High quartz contents correlate with high  $\text{SiO}_2$  contents. Plagioclase and amphibole show a strong correlation, indicating that they may be delivered from the same source rocks. Likewise, quartz and the feldspar minerals correlate positively.

#### 4.4. Source Rock Discrimination and Mixing Modeling

The first two principal components, explaining ca. 81% of the source rock data variability, essentially reveal three clusters: The clastic rock samples, characterized by  $\text{SiO}_2$ ,  $\text{Al}_2\text{O}_3$ ,  $\text{K}_2\text{O}$ ,  $\text{P}_2\text{O}_5$ ,  $\text{Fe}_2\text{O}_3$ , and  $\text{TiO}_2$ , plot in the lower right quadrant. Diorite, gabbro, and amphibolite samples plot in the lower left quadrant and are chiefly characterized by MnO, MgO, and CaO. The granodiorite, granite, and gneiss samples form the most variable cluster in the upper two quadrants and are characterized by  $\text{Na}_2\text{O}$ ,  $\text{Al}_2\text{O}_3$ , and  $\text{K}_2\text{O}$ . The three loess samples do not form a distinguishable cluster. Accordingly, the source rock categories clastic, gabbro/diorite/amphibolite, and granitoid/gneiss were

used for the mixing model. The river sediment plots between the three source rock clusters (Figure 10), which confirms that it may be indeed a mixture of the three considered main source rocks.

The mixing modeling results change significantly between different grain-size fractions and tend to be overall similar within each grain-size class (Figure 11). One exception is the bulk Gersprenz February 2020 sample, which contains mostly fine-grained suspended sediment deposited on the sand bar during a flood event. Although the bulk sample is compositionally different from the other bulk samples (Figure 11), its narrow grain-size fractions are comparable with the grain-size fractions of other samples. Overall, the Gersprenz river samples show a dominance of the granitoid/gneiss source in the grain-size fractions  $-1-0$  and  $0-1$   $\Phi$ , and increasing contributions of the diorite/gabbro/amphibolite and clastic source in the finer grain-size fractions. For the Mümling river, the mixing model predicts a dominance of the clastic source in all samples, and a minor contribution of the granitoid/gneiss source and the diorite/gabbro/amphibolite source in the finest grain sizes  $>4$  and  $3-4$   $\Phi$ . The results for the Modau river indicate a mixed contribution of all three sources in the coarser grain-size fractions ( $-1-0$  and  $0-1$   $\Phi$ ). The predicted contribution of the sedimentary source increases systematically with decreasing grain size at the expense of the granitoid/gneiss source. The diorite/gabbro/amphibolite source contribution stays relatively constant. Overall, the mixing model predicts similar source contributions in the finest fraction ( $>4$   $\Phi$ ) for all three catchments despite different bedrock geology.

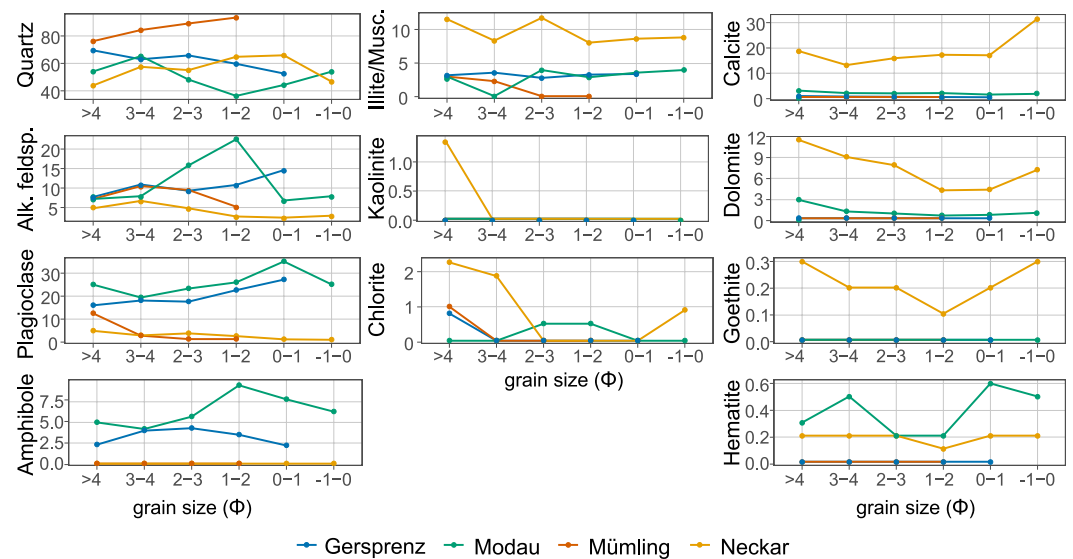


**Figure 8.** Variability of sediment mineralogy depending on the analyzed grain-size fraction ( $\Phi$  scale). Y-axis is in %. Note that some mineral concentrations were below the detection limit, and these minerals are given with 0% here.

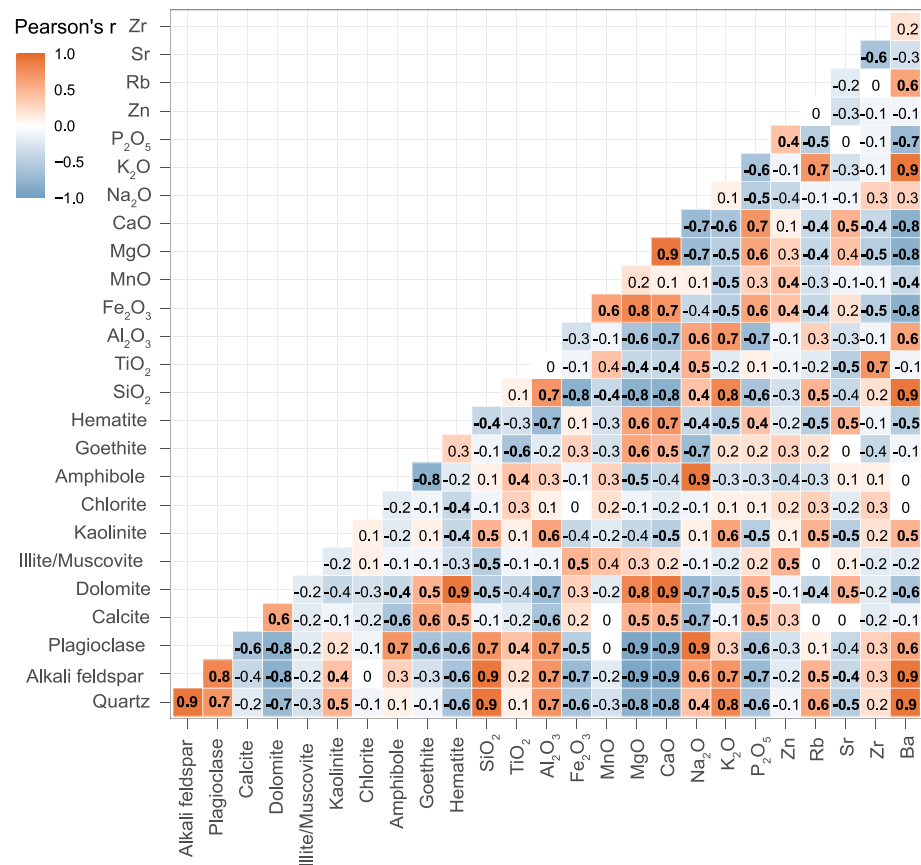


**Figure 9.** Correlation matrix of element and mineral pairs based on Pearson's  $r$ . The data were log-ratio transformed to eliminate artificial correlation effects due to the constant sum problem. Statistically significant correlations ( $p$ -values < 0.05) are indicated with bold numbers.

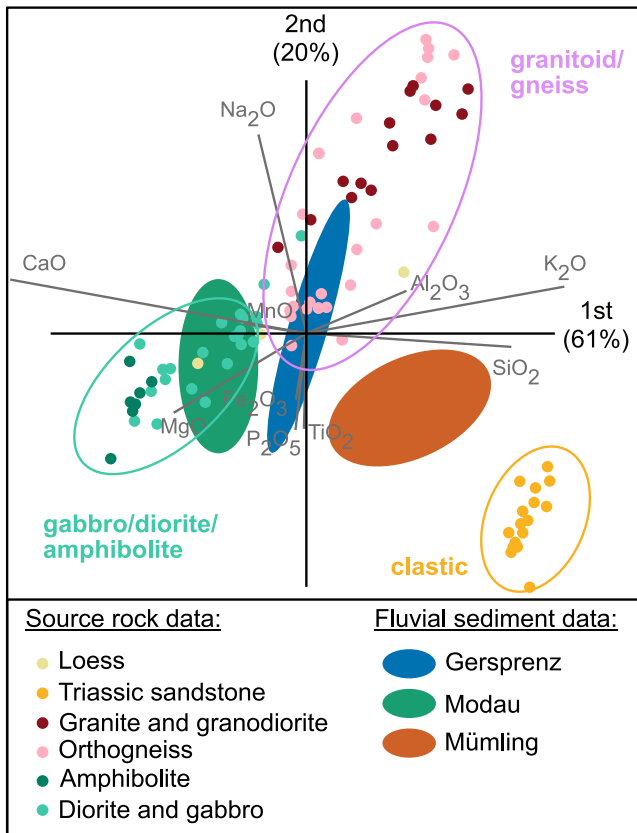


**Figure 10.** Principal component analysis based on major element oxide concentrations of the compiled source rock data and the fluvial sand data from Figure 6. Source rock data for the clastic rocks (Buntsandstein Group) from Soyk (2015). Source rock data for the crystalline Odenwald rocks from Altenberger and Besch (1993), Altenberger et al. (1990), Altherr et al. (1999), Poller et al. (2001), Reischmann et al. (2001), Siebel et al. (2012), Will et al. (2015), Will et al. (2021), and Will and Schmädicke (2001).

## 5. Discussion

The clear differences in sediment mineralogy and geochemistry between the four studied rivers (Figure 6) can qualitatively be explained by different catchment bedrock geology (Figure 1). The high CaO and carbonate content in the Neckar river sediment is related to the abundance of lime- and dolostone in the catchment. High SiO<sub>2</sub> and quartz contents in the Mümling catchment result from the composition of the source rock being mostly quartz-rich. The similarity of the Gersprenz and Modau sand stems from an overall similar catchment geology dominated by plutonic and metamorphic rocks. High Na<sub>2</sub>O and K<sub>2</sub>O contents point to high feldspar contents of (meta-)granitoid rocks, whereas amphibole may be derived from the amphibolites, diorites, or granodiorites that are common in these two catchments (Altherr et al., 1999; Stein, 2001).

The quantitative mixing modeling overall confirms that sediment composition is controlled by the main bedrock lithologies considered in this study. The mixing model predicts a dominant contribution of the granitoid/gneiss source in the Gersprenz river samples, a dominant contribution of the clastic source in the Mümling river, and a mixed contribution of granitoid/gneiss and diorite/gabbro/amphibolite rocks in the Modau river (Figure 11). These predictions are overall in good agreement with the observed area percentage covered by these sources, which suggests that erosion in the studied catchments is spatially rather uniform and that all sources supply sand-sized detritus. The predicted relative contribution by the three sources is similar within the same grain-size class, which indicates that it is temporally stable and that there are no significant provenance changes over the year. The exceptional Gersprenz February 2020 sample demonstrates that even during extreme events, the provenance of suspended and bedload material does not change substantially in this river. Time series from the Rhine river (van der Perk & Espnoza Vilches, 2020) and the Amazon, Orinoco, and Maroni rivers (Rousseau et al., 2019), in contrast, have identified source changes based on suspended sediment chemistry. This might be related to their large catchment sizes and consequently higher spatial dynamics, and/or to the generally faster transport time (and therefore signal transfer time) of suspended compared to bedload sediment (Tofelde et al., 2021).

The mixing model predicts different source rock contributions in different grain sizes, which is a result of a strong granulometric control on sediment composition (Figure 6). The variability of chemistry and mineralogy between

different size fractions of one sample is governed by three factors: A size-density sorting effect by which dense minerals are preferably found in fine grain-size fractions (Garzanti et al., 2008; Jonell et al., 2018), the original size of minerals in the source rocks (Hatzenbühler et al., 2022; Weltje et al., 2018), and physical and chemical weathering that break down minerals and enrich fine-grained weathering products in the finer grain-size fractions (Le Pera et al., 2001; von Eynatten et al., 2012, 2016).

### 5.1. Size-Density Sorting Effect

The highest chemical variability was observed in the bulk and >4  $\Phi$  subsamples (Figure 5), which is caused by the wider range of grain sizes comprised in these fractions as compared to the narrower grain-size fractions (1  $\Phi$  intervals). However, the narrow grain-size fractions also show compositional variability over the year with average relative standard deviations of ca. 15%. Some of this variability is probably related to analytical uncertainty, especially for elements with relatively high errors (e.g., Ba, Zr), but given the different orders of magnitude of uncertainty and variability, natural controls are likely as well. We interpret the higher variability of TiO<sub>2</sub>, MnO, P<sub>2</sub>O<sub>5</sub>, Zn, and Zr to express temporally variable concentrations of heavy minerals. Depending on the local hydraulic conditions in the river, less dense minerals are easier entrained by the stream (selective entrainment), which can cause the enrichment of heavy minerals up to the formation of placer deposits

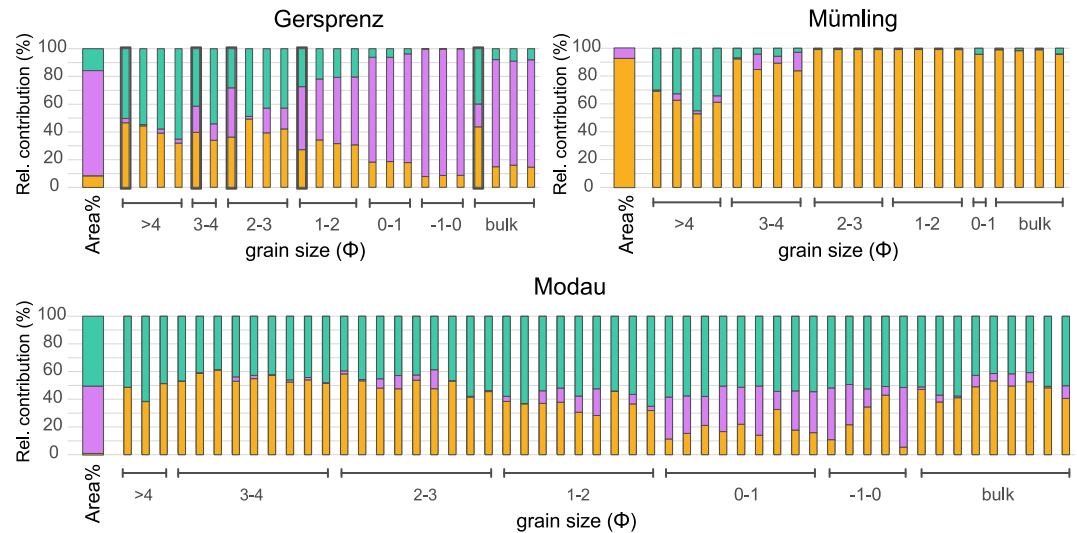


**Figure 11.** Mixing modeling results for the three Odenwald rivers displaying the relative contribution of the three considered source rocks. The columns to the left display the area percentage of the three sources in each catchment (normalized to 100% for not considered lithologies such as carbonates and Quaternary cover). The bold boxes around some of the Gersprenz samples indicate the February 2020 sediment that was deposited during the flooding of the sand bar from suspended load.

(Garzanti et al., 2009; Komar, 2007; Slingerland, 1977). Our results suggest that hydrodynamic conditions and the resulting heavy mineral concentrations vary even at the same sampling location at different times of the year, whereas elements not associated with heavy minerals tend to be less variable (Figure 5).

We interpret the increase of  $P_2O_5$ ,  $TiO_2$ , and Zr concentrations with decreasing grain size as an expression of the heavy minerals apatite,  $TiO_2$  polymorphs (e.g., rutile, anatase), and zircon, respectively, that tend to be enriched in finer grain-size fractions than less dense minerals (Garzanti et al., 2008; Liu et al., 2019; von Eynatten et al., 2012). Likewise,  $Fe_2O_3$ , MnO, and Zn, which show higher concentrations in finer grain size-fractions, are probably bound to dense minerals.  $Fe_2O_3$  is present in ferrous silicate heavy minerals such as amphiboles and pyroxenes, or in primary or secondary iron oxides and hydroxides that also tend to be enriched in finer grain-size fractions. We favor the association of iron with silicate heavy minerals since the XRD data show high amounts of amphiboles but insignificant amounts of iron oxide minerals (Figure 8). MnO might be associated with carbonates, Fe- and Mn-bearing oxides or some silicate heavy minerals (e.g., spessartine-rich garnet, tourmaline, epidote group). In our case, MnO shows no correlation with CaO or MgO, but a strong correlation with  $Fe_2O_3$ ,  $TiO_2$ , and  $P_2O_5$ , suggesting that Mn is not carbonate-bound, but associated with silicate heavy minerals or iron oxides. Likewise, Zn is correlated with  $Fe_2O_3$ , MnO,  $TiO_2$ , and  $P_2O_5$ , suggesting a similar association with dense minerals such as magnetite (Johnson, 1994).

## 5.2. Weathering Intensity

In settings with pronounced chemical weathering, feldspar contents tend to decrease with decreasing grain size, while weathering products such as clay minerals increase with decreasing grain size (von Eynatten et al., 2016). In settings with limited chemical weathering, this trend might be less pronounced or even the opposite because feldspars break down along their cleavage planes due to mechanical abrasion (Basu, 1976; Heins, 1993). In our study, we observed both trends, suggesting differences in weathering regime between the crystalline rock-dominated Gersprenz and Modau (decreasing plagioclase contents with decreasing grain size) and the sedimentary rock-dominated Mümling and Neckar (increasing plagioclase contents with decreasing grain size). Likewise, chemical indices such as the CIX are thought to reflect chemical weathering intensity (Buggle et al., 2011; Nesbitt & Young, 1984). Hohberger and Einsele (1979) calculated ratios of dissolved to mechanical river load of approximately 1:1 for southern German river catchments, indicating significant chemical weathering. However, the dissolved load is probably derived from carbonate weathering rather than silicate weathering, which the CIX (and other traditional weathering indices) are not sensitive to. In our case, the CIX values differ between the four rivers, which would suggest that the Neckar sediment is the most and



the Mümling sediment the least weathered (Figure 7a). However, there are no significant differences in the four river catchments regarding mean temperature, precipitation, or land use (Table 1) that would explain differences in CIX values or different plagioclase weathering behavior. In addition to weathering intensity, such indicators heavily depend on the source rock composition (Garzanti & Resentini, 2016; Nesbitt & Young, 1984), grain size (Hatano et al., 2019), and original texture and mineral sizes in the source rocks (Hatzembühler et al., 2022; Heins, 1993; Weltje et al., 2018).

The CIX value difference between Mümling and Neckar sediment can readily be explained by the higher CIX values in the Keuper sandstone that is common in the Neckar catchment compared to the relatively low CIX values in the Buntsandstein sandstone, which is the dominant source rock in the Mümling catchment. We interpret this with a higher weathering intensity during the more humid climate of the Late Triassic (Keuper) compared to the Early Triassic (Buntsandstein) as shown by facies associations (Hornung & Aigner, 2002; Hug, 2004) and climate-proxy evidence (Reinhard & Ricken, 2000). Additionally, the higher CIX in the Keuper sandstone samples may be caused by the presence of kaolinite cement formed during (early) diagenesis (Hornung & Aigner, 1999; Kulke, 1969), which is supported by the occurrence of kaolinite in the mud of the Neckar river (Figure 8). Consequently, we interpret the CIX values to reflect past (near-) surface weathering or eogenetic conditions rather than modern weathering intensity. The CIX values of the Gersprenz and Modau river sediments draining the Odenwald complex are close to (or even slightly lower than) the median values of the considered source rocks, suggesting little overall modification of the sediment composition by chemical weathering. The decrease of plagioclase content with decreasing grain size in the Gersprenz and Modau river sediment instead reflects the rather coarse-grained plagioclase minerals in the granitoid source rock and limited weathering.

Further evidence for minor chemical silicate weathering is provided by the overall low percentage of clay minerals in the river sediment (Figure 8), particularly in the finest analyzed fraction. Chlorite is probably detrital in origin as it occurs as a ubiquitous alteration product of biotite (and amphibole) in crystalline rocks in the Odenwald (Stein et al., 2022; Will & Schmädicke, 2003) and as an authigenic phase in the Keuper and Buntsandstein sandstones (Clauer et al., 2008; Krumm, 1969). Kaolinite was detected only in the mud of the Neckar river, where it can be explained by its presence as a diagenetic mineral in the Keuper sandstone source (Hornung & Aigner, 1999; Kulke, 1969). Illite/muscovite only increases with decreasing grain size in the Mümling sediment, which could point toward the enrichment of illite as a weathering product in the fine grain sizes. However, it might also be derived from the recycling of Buntsandstein sandstones with fine-grained illite cement and illite-bearing clay intraclasts (Hug, 2004; Soyk, 2015). In any case, the illite/muscovite concentration of generally <5 wt% in the Mümling sediment is low compared to illite contents in high-intensity weathering settings (von Eynatten et al., 2016). In all other rivers, illite/muscovite is present in roughly similar proportions in all grain-size fractions, suggesting that they do not occur as (usually very fine-grained) secondary minerals but are instead part of larger particles such as rock fragments and therefore of detrital origin. All these arguments point toward negligible control of modern chemical weathering and dominance of physical weathering (Heins, 1993; Kautz & Martin, 2007).

### 5.3. Source Rock Contributions

In the absence of intense chemical weathering, the large variability of source rock contribution in different grain sizes can be explained by three effects:

1. Source rock effect: Some lithologies (e.g., fine-grained siliciclastic rock or amphibolite) may produce finer-grained detritus than others (e.g., granitoid rock) due to the source rock grain size and/or mechanical behavior during physical weathering.
2. Hydraulic effect: Two of the three source rocks, the diorite/gabbro/amphibolite, and the clastic sources, are characterized by high concentrations of heavy mineral-bound elements. The diorite/gabbro/amphibolite source is expected to have higher heavy mineral fertility than siliciclastic rock (Garzanti et al., 2009), which could result in an overprediction of diorite/gabbro/amphibolite detritus in finer grain sizes. This hydraulic effect is possibly amplified because the compositional difference between finer grain sizes is smaller than for coarser grain sizes (Figure 6), which influences the performance of the mixing model.
3. Database effect: There may be additional sediment sources we have not considered in this mixing model due to missing source rock data, and the model thus attributes certain contributions to the chemically closest but wrong source rock class.

In the Gersprenz river, the mixing model predicts a higher contribution by the diorite/gabbro/amphibolite as well as the clastic source in the finer-grained samples than in the coarser-grained samples. Both the source rock effect and the hydraulic effect seem plausible explanations since we observe increasing contents of elements such as MgO, P<sub>2</sub>O<sub>5</sub>, TiO<sub>2</sub>, and Fe<sub>2</sub>O<sub>3</sub> in the finer grain-size fractions (Figure 4). Similarly, the model predicts a higher diorite/gabbro/amphibolite contribution in the Mümling river. However, the catchment of the Mümling river is dominated by clastic rocks and mafic rocks are not exposed. As in the Gersprenz, we observe an increase of MnO and MgO in the finer grain sizes of the Mümling samples (Figure 4), pointing toward a hydraulic control. However, in the Mümling drainage area, there are minor occurrences of mud and carbonate rocks that could contribute to MnO and MgO and that we did not consider in the mixing model (database effect). The results for the Modau indicate an overall higher contribution of the diorite/gabbro/amphibolite source than in the other two rivers, which is plausible given that around half of the catchment area is covered by this type of rock (Figures 1 and 11). The contribution of the granitoid source decreases with decreasing grain size, which we interpret as a source rock effect with overall coarse-grained detritus supplied by the granitoid source. The model also predicts a clastic contribution in the finer grain sizes, which we interpret as a database effect. There is only a very small percentage of pre-Quaternary sedimentary rocks present in the Modau catchment, and it seems quite unlikely that they contribute over 50% to the river sediment. However, sediment could be delivered by loess and other Quaternary sediment because they cover around a third of the catchment area (Figures 1 and 11), are quite erodible due to lack of cement, and tend to deliver silt- or fine-sand fractions (Pflanz et al., 2022). Although the three loess samples from the Modau catchment considered in this study are not particularly similar to the sedimentary clastic source (Figure 10), loess remains the most likely sediment source, and more data are needed to test this hypothesis.

## 6. Conclusions

The composition of bulk fluvial bedload sediment changes over a short observation period in all four studied river basins. This is primarily caused by variations in grain-size distribution rather than changes in source contributions. Especially extreme events, such as the February 2020 flood in the Gersprenz catchment, can cause bulk sediment compositions that are not representative. However, even narrow grain size compositions show temporal variability in response to hydrodynamics and the resulting enrichment or depletion of heavy minerals. This has been noted in other studies (e.g., Bouchez et al., 2011), but the quantification of selective entrainment as a function of flow strength and transport capacity remains challenging, especially for bedload sediment (Komar, 2007; Slingerland, 1977). In addition, sediment composition changes significantly with grain size due to source rock texture and sorting effects (Garzanti et al., 2009; Jonell et al., 2018; von Eynatten et al., 2012). Consequently, neither bulk sediment nor narrow grain-size fractions necessarily provide an averaged composition reflecting typical erosional and depositional processes in the catchment area. However, using a combination of methods (geochemistry, mineralogy, granulometry) on multiple samples and multiple narrow grain-size fractions enables disentangling the different processes controlling sediment composition and the reasons responsible for its temporal variability (Jonell et al., 2018). The importance of time-series analysis was also demonstrated by Rousseau et al. (2019) and van der Perk and Espinoza Vilches (2020), who used a similar approach for suspended sediment. Where such detailed sampling over several months is not possible due to practical (e.g., temporal or financial) reasons, an average temporal geochemical variability of 15%–20% should be taken into consideration. Our recommendation for sediment fingerprinting and mixing modeling of source rock contributions with geochemical data is to use several narrow grain sizes to reduce the effects of temporal and granulometric variability. The selection of specific grain-size fraction(s) for mixing modeling requires knowledge of source rock composition and texture, as some (e.g., volcanic) source rocks may not supply significant amounts of sand-sized detritus to the bedload (e.g., Hatzenbühler et al., 2022). In our case, however, coarse grain sizes (<1  $\Phi$ ) gave more realistic source rock contributions, approximately equal to their areal distribution in the catchments, than fine grain sizes (>3  $\Phi$ ). Particularly, the finest fraction (>4  $\Phi$ ) yielded similar predicted source contributions (ca. 50:50 of clastic and diorite/gabbro/amphibolite sources) for the three considered catchments despite obvious lithological differences in their bedrock geology.

## Data Availability Statement

The data of this paper (Stutenbecker et al., 2023) are available in the PANGAEA data repository: <https://doi.pangaea.de/10.1594/PANGAEA.959006>.

## Acknowledgments

We thank Andrea Madella for assistance during sampling, Gabriela Schubert and Ariane Djahansouzi for help during sample preparation. Carita Augustsson, Sebastien Bertrand, and a third anonymous reviewer provided constructive and helpful reviews. Open Access funding enabled and organized by Projekt DEAL.

## References

- Altenberger, U., & Besch, T. (1993). The Böllstein Odenwald: Evidence for pre- to early Variscan plate convergence in the Central European Variscides. *Geologische Rundschau*, 82(3), 475–488. <https://doi.org/10.1007/BF00212411>
- Altenberger, U., Besch, T., Mocek, B., Zaipeng, Y., & Yong, S. (1990). Geochemie und Geodynamik des Böllsteiner Odenwaldes. *Mainzer Geowissenschaftliche Mitteilungen*, 19, 183–200.
- Altherr, R., Henes-Klaiber, U., Hegner, E., Satir, M., & Langer, C. (1999). Plutonism in the Variscan Odenwald (Germany): From subduction to collision. *International Journal of Earth Sciences*, 88(3), 422–443. <https://doi.org/10.1007/s005310050276>
- Amann, B., Bertrand, S., Alvarez-Garretón, C., & Reid, B. (2022). Seasonal variations in fjord sediment grain size: A pre-requisite for hydrological and climate reconstructions in partially glacierized watersheds (Baker River, Patagonia). *Journal of Geophysical Research: Earth Surface*, 127, 2. <https://doi.org/10.1029/2021JF006391>
- Basu, A. (1976). Petrology of Holocene fluvial sand derived from plutonic source rocks: Implications to paleoclimatic interpretation. *Journal of Sedimentary Petrology*, 46(3), 694–709. <https://doi.org/10.1306/212F7031-2B24-11D7-8648000102C1865D>
- Berger, C., McArdeil, B. W., & Schlunegger, F. (2011). Sediment transfer patterns at the Illgraben catchment, Switzerland: Implications for the time scales of debris flow activities. *Geomorphology*, 125(3), 421–432. <https://doi.org/10.1016/j.geomorph.2010.10.019>
- Bouchez, J., Gaillardet, J., France-Lanord, C., Maurice, L., & Dutra-Maia, P. (2011). Grain size control of river suspended sediment geochemistry: Clues from Amazon River depth profiles. *Geochemistry, Geophysics, Geosystems*, 12(3), Q03008. <https://doi.org/10.1029/2010GC003380>
- Buggle, B., Glaser, B., Hambach, U., Gerasimenko, N., & Marković, S. (2011). An evaluation of geochemical weathering indices in loess-paleosol studies. *Quaternary International*, 240(1–2), 12–21. <https://doi.org/10.1016/j.quaint.2010.07.019>
- Caracciolo, L. (2020). Sediment generation and sediment routing systems from a quantitative provenance analysis perspective: Review, application and future development. *Earth-Science Reviews*, 209, 103226. <https://doi.org/10.1016/j.earscirev.2020.103226>
- Carter, J., Walling, D. E., Owens, P. N., & Leeks, G. J. L. (2006). Spatial and temporal variability in the concentration and speciation of metals in suspended sediment transported by the River Aire, Yorkshire, UK. *Hydrological Processes*, 20(14), 3007–3027. <https://doi.org/10.1002/hyp.6156>
- Clauer, N., Liewig, N., Ledesert, B., & Zwingmann, H. (2008). Thermal history of Triassic sandstones from the Vosges Mountains-Rhine Graben rift area, NE France, based on K-Ar illite dating. *Clay Minerals*, 43(3), 363–379. <https://doi.org/10.1180/claymin.2008.043.3.03>
- Cohen, S., Kettner, A. J., & Syvitski, J. P. M. (2014). Global suspended sediment and water discharge dynamics between 1960 and 2010: Continental trends and intra-basin sensitivity. *Global and Planetary Change*, 115, 4458–58. <https://doi.org/10.1016/j.gloplacha.2014.01.011>
- Collins, A. L., Walling, D. E., & Leeks, G. J. L. (1996). Composite fingerprinting of the spatial source of fluvial suspended sediment: A case study of the Exe and Severn River basins, United Kingdom. *Géomorphologie: Relief, Processus, Environnement*, 2(2), 41–53. <https://doi.org/10.3406/morfo.1996.877>
- Cornes, R., van der Schrier, G., van den Besselaar, E. J. M., & Jones, P. D. (2018). An ensemble version of the E-OBS temperature and precipitation datasets. *Journal of Geophysical Research: Atmospheres*, 123(17), 9391–9409. <https://doi.org/10.1029/2017JD028200>
- Douglas, G. B., Ford, P. W., Palmer, M. R., Noble, R. M., Packett, R. J., & Krull, E. S. (2008). Fitzroy River Basin, Queensland, Australia. IV. Identification of flood sediment sources in the Fitzroy River. *Environmental Chemistry*, 5(3), 243–257. <https://doi.org/10.1071/EN07091>
- Federal Institute for Geosciences and Natural Resources, Germany (Bundesanstalt für Geologie und Rohstoffe). (2007). The general geological map of the Federal Republic of Germany 1:200,000 (GÜK200). Retrieved from [https://www.bgr.bund.de/EN/Themen/Sammlungen-Grundlagen/GG\\_geol\\_Info/Karten/Deutschland/GUEK200/guek200\\_node\\_en.html;jsessionid=4E8E74A32EE36C7643246F47FEE935ED.internet012](https://www.bgr.bund.de/EN/Themen/Sammlungen-Grundlagen/GG_geol_Info/Karten/Deutschland/GUEK200/guek200_node_en.html;jsessionid=4E8E74A32EE36C7643246F47FEE935ED.internet012)
- Florsheim, J. L., Pellerin, B. A., Oh, N. H., Ohara, N., Bachand, P. A. M., Bachand, S. M., et al. (2011). From deposition to erosion: Spatial and temporal variability of sediment sources, storage, and transport in a small agricultural watershed. *Geomorphology*, 132(3–4), 272–286. <https://doi.org/10.1016/j.geomorph.2011.04.037>
- Garzanti, E., Andò, S., & Vezzoli, G. (2008). Settling equivalence of detrital minerals and grain-size dependence of sediment composition. *Earth and Planetary Science Letters*, 273(1–2), 138–151. <https://doi.org/10.1016/j.epsl.2008.06.020>
- Garzanti, E., Andò, S., & Vezzoli, G. (2009). Grain-size dependence of sediment composition and environmental bias in provenance studies. *Earth and Planetary Science Letters*, 277(3–4), 422–432. <https://doi.org/10.1016/j.epsl.2008.11.007>
- Garzanti, E., & Resentini, A. (2016). Provenance control on chemical indices of weathering (Taiwan river sands). *Sedimentary Geology*, 336, 81–95. <https://doi.org/10.1016/j.sedgeo.2015.06.013>
- Garzanti, E., Vermeesch, P., Padoan, M., Resentini, A., Vezzoli, G., & Andò, S. (2014). Provenance of passive-margin sand (southern Africa). *The Journal of Geology*, 122(1), 17–42. <https://doi.org/10.1086/674803>
- Garzanti, E., Vezzoli, G., Andò, S., Lavé, J., Attal, M., France-Lanord, C., & DeCelles, P. (2007). Quantifying sand provenance and erosion (Marsyandi River, Nepal Himalaya). *Earth and Planetary Science Letters*, 258(3–4), 500–515. <https://doi.org/10.1016/j.epsl.2007.04.010>
- Hatano, N., Yoshida, K., & Sasao, E. (2019). Effects of grain size on the chemical weathering index: A case study of Neogene fluvial sediments in southwest Japan. *Sedimentary Geology*, 386, 1–8. <https://doi.org/10.1016/j.sedgeo.2019.03.017>
- Hatzenbühler, D., Caracciolo, L., Weltje, G. J., Piraquive, A., & Regelous, M. (2022). Lithologic, geomorphic, and climatic controls on sand generation from volcanic rocks in the Sierra Nevada de Santa Marta massif (NE Colombia). *Sedimentary Geology*, 429, 106076. <https://doi.org/10.1016/j.sedgeo.2021.106076>
- Heins, W. A. (1993). Source rock texture versus climate and topography as controls on the composition of modern, plutoniclastic sand. Geological Society of America Special Paper. In M. J. Johnson & A. Basu (Eds.), *Processes controlling the composition of clastic sediment* (Vol. 284, pp. 135–146).
- Hessian Agency for Nature Conservation, Environment and Geology. (2020). Water level and discharge of the rivers Gersprenz, Modau, and Mümling at the gauging stations Harreshausen, Hainstadt, and Eberstadt. Retrieved from <https://www.hlnug.de/static/pegel/wikiweb2/>
- Hohberger, K., & Einsele, G. (1979). Die Bedeutung des Lössabtrags verschiedener Gesteine für die Landschaftsentwicklung in Mitteleuropa. *Zeitschrift für Geomorphologie*, 23, 361–382.
- Hornung, J., & Aigner, T. (1999). Reservoir and aquifer characterization of fluvial architectural elements: Stubensandstein, Upper Triassic, southwest Germany. *Sedimentary Geology*, 129(3–4), 215–280. [https://doi.org/10.1016/S0037-0738\(99\)00103-7](https://doi.org/10.1016/S0037-0738(99)00103-7)

- Hornung, J., & Aigner, T. (2002). Reservoir architecture in a terminal alluvial plain: An outcrop analogue study (upper Triassic, southern Germany). Part 1: Sedimentology and petrophysics. *Journal of Petroleum Geology*, 25(1), 3–30. <https://doi.org/10.1111/j.1747-5457.2002.tb00097.x>
- Hug, N. (2004). Sedimentgenese und Paläogeographie des höheren Zechstein bis zur Basis des Buntsandstein in der Hessischen Senke. In *Geologische Abhandlungen Hessen* (Vol. 113). Hessisches Landesamt für Naturschutz, Umwelt und Geologie.
- Ingersoll, R. V., Bullard, T. F., Ford, R. L., Grimm, J. P., Pickle, J. D., & Sares, S. W. (1984). The effect of grain size on detrital modes: A test of the Gazzi-Dickinson point-counting method. *Journal of Sedimentary Petrology*, 54, 0103–0116. <https://doi.org/10.1306/212F83B9-2B24-11D7-8648000102C1865D>
- Johnson, C. A. (1994). Partitioning of zinc among common ferromagnesian minerals and implications for hydrothermal mobilization. *The Canadian Mineralogist*, 32, 121–132.
- Jonell, T. N., Li, Y., Blusztajn, J., Giosan, L., & Clift, P. D. (2018). Signal or noise? Isolating grain size effects on Nd and Sr isotope variability in Indus delta sediment provenance. *Chemical Geology*, 485, 56–73. <https://doi.org/10.1016/j.chemgeo.2018.03.036>
- Kautz, C. Q., & Martin, C. E. (2007). Chemical and physical weathering in New Zealand's Southern Alps monitored by bedload sediment major element composition. *Applied Geochemistry*, 22(8), 1715–1735. <https://doi.org/10.1016/j.apgeochem.2007.03.031>
- Komar, P. D. (2007). The entrainment, transport and sorting of heavy minerals by waves and currents. Developments in Sedimentology. In M. A. Mange & D. T. Wright (Eds.), *Heavy minerals in use* (Vol. 58, pp. 3–48). Elsevier. [https://doi.org/10.1016/S0070-4571\(07\)58001-5](https://doi.org/10.1016/S0070-4571(07)58001-5)
- Krumm, H. (1969). A scheme of clay mineral stability in sediments, based on clay mineral distribution in Triassic sediments of Europe. In *Proceedings of the international clay conference Tokyo* (pp. 313–324). Israel Universities Press.
- Kulke, H. (1969). Petrographie und Diagenese des Stubensandsteins (mittlerer Keuper) aus Tiefbohrungen im Raum Memmingen (Bayern). *Contributions to Mineralogy and Petrology*, 20(2), 135–163. <https://doi.org/10.1007/BF00399628>
- Landesanstalt für Umwelt Baden-Württemberg. (2020). Water level and discharge of the Neckar river at the gauging station Horb. Retrieved from <https://udo.lubw.baden-wuerttemberg.de/public/>
- Lane, S. N., Bakker, M., Costa, A., Girardclos, S., Loizeau, J.-L., Molnar, P., et al. (2019). Making stratigraphy in the Anthropocene: Climate change impacts and economic conditions controlling the supply of sediment to Lake Geneva. *Scientific Reports*, 9(1), 8904. <https://doi.org/10.1038/s41598-019-44914-9>
- Le Pera, E., Arribas, J., Critelli, S., & Tortosa, A. (2001). The effects of source rocks and chemical weathering on the petrogenesis of siliciclastic sand from the Neto River (Calabria, Italy): Implications for provenance studies. *Sedimentary Geology*, 48(2), 357–378. <https://doi.org/10.1046/j.1365-3091.2001.00368.x>
- Littke, R., Scheck-Wenderoth, M., Brix, M. R., & Nelskamp, S. (2008). Subsidence, inversion and evolution of the thermal field. In R. Littke, U. Bayer, D. Gajewski, & S. Nelskamp (Eds.), *Dynamics of complex intracontinental basins: The Central European basin system* (pp. 125–154). Springer.
- Litty, C., Duller, R., & Schlunegger, F. (2016). Paleohydraulic reconstruction of a 40 ka-old terrace sequence implies that water discharge was larger than today. *Earth Surface Processes and Landforms*, 41(7), 884–898. <https://doi.org/10.1002/esp.3872>
- Liu, D., Bertrand, S., Vandekerckhove, E., & Renson, V. (2022). Provenance of Baker River sediments (Chile, 48°S): Implications for the identification of flood deposits in fjord sediments. *Earth Surface Processes and Landforms*, 47(3), 825–838. <https://doi.org/10.1002/esp.5287>
- Liu, D., Bertrand, S., & Weltje, G. J. (2019). An empirical method to predict sediment grain size from inorganic geochemical measurements. *Geochemistry, Geophysics, Geosystems*, 20(7), 3690–3704. <https://doi.org/10.1029/2018GC008154>
- Lizaga, I., Latorre, B., Gaspar, L., & Navas, A. (2020). FingerPro: An R package for tracking the provenance of sediment. *Water Resources Management*, 34(12), 3879–3894. <https://doi.org/10.1007/s11269-020-02650-0>
- Müller, G., Middelburg, J. J., & Sluijs, A. (2021). Introducing GloRiSe – A global database on river sediment composition. *Earth System Science Data*, 13(7), 3565–3575. <https://doi.org/10.5194/essd-13-3565-2021>
- Navrátil, O., Evrard, O., Esteves, M., Legout, C., Ayrault, S., Némery, J., et al. (2012). Temporal variability of suspended sediment sources in an alpine catchment combining river/rainfall monitoring and sediment fingerprinting. *Earth Surface Processes and Landforms*, 37(8), 828–846. <https://doi.org/10.1002/esp.3201>
- Navrátil, T., Rohovec, J., & Žák, K. (2008). Floodplain sediments of the 2002 catastrophic flood at the Vltava (Moldau) River and its tributaries: Mineralogy, chemical composition, and post-sedimentary evolution. *Environmental Geology*, 56(2), 399–412. <https://doi.org/10.1007/s00254-007-1178-8>
- Nesbitt, H. W., & Young, G. M. (1982). Early Proterozoic climates and plate motions inferred from major element chemistry of lutites. *Nature*, 299(5885), 715–717. <https://doi.org/10.1038/299715a0>
- Nesbitt, H. W., & Young, G. M. (1984). Prediction of some weathering trends of plutonic and volcanic rocks based on thermodynamic and kinetic considerations. *Geochimica et Cosmochimica Acta*, 48(7), 1523–1534. [https://doi.org/10.1016/0016-7037\(84\)90408-3](https://doi.org/10.1016/0016-7037(84)90408-3)
- Peters, G., & van Balen, R. (2007). Pleistocene tectonics inferred from fluvial terraces of the northern Upper Rhine Graben, Germany. *Tectonophysics*, 430(1–4), 41–65. <https://doi.org/10.1016/j.tecto.2006.10.008>
- Pflanz, D., Kunz, A., Hornung, J., & Hinderer, M. (2022). New insights into the age of aeolian sand deposition in the Upper Rhine Graben (Germany). *Quaternary International*, 625, 1–13. <https://doi.org/10.1016/j.quaint.2022.03.019>
- Poller, U., Altenberger, U., & Schubert, W. (2001). Geochemical investigations of the Bergsträsser Odenwald amphibolites – Implications for back-arc magmatism. *Mineralogy and Petrology*, 72(1–3), 63–76. <https://doi.org/10.1007/s007100170027>
- R Core Team. (2021). *R: A language and environment for statistical computing*. Vienna, Austria: R Foundation for Statistical Computing. <https://www.R-project.org/>
- Reinhard, L., & Ricken, W. (2000). Climate cycles documented in a playa system: Comparison of geochemical signatures derived from subbasins (Triassic, Middle Keuper, German Basin). In H. Bock, R. Müller, R. Swennen, & W. Zimmerle (Eds.), *West European case studies in stratigraphy, Zentralblatt für Geologie und Paläontologie part I* (Vol. 3/4, pp. 315–340). E. Schweizerbart'sche Verlagsbuchhandlung.
- Reischmann, T., Anthes, G., Jaeckel, P., & Altenberger, U. (2001). Age and origin of the Böllsteiner Odenwald. *Mineralogy and Petrology*, 72(1–3), 29–44. <https://doi.org/10.1007/s007100170025>
- Riembauer, G., Weinmann, A., Xu, S., Eichfuss, S., Eberz, C., & Neteler, M. (2021). Germany-wide Sentinel-2 based land cover classification and change detection for settlement and infrastructure monitoring. 2021 conference on big data from space (BiDS'2021).
- Romans, B. W., Castellort, S., Covault, J. A., Fildani, A., & Walsh, J. P. (2016). Environmental signal propagation in sedimentary systems across timescales. *Earth-Science Reviews*, 153, 7–29. <https://doi.org/10.1016/j.earscirev.2015.07.012>
- Rousseau, T. C. C., Roddaz, M., Moquet, J.-S., Handt Delgado, H., Calves, G., & Bayon, G. (2019). Controls on the geochemistry of suspended sediments from large tropical South American rivers (Amazon, Orinoco and Maroni). *Chemical Geology*, 522, 38–54. <https://doi.org/10.1016/j.chemgeo.2019.05.027>



- Schillereff, D. N., Chiverell, R. C., Macdonald, N., & Hooke, J. M. (2014). Flood stratigraphies in lake sediments: A review. *Earth-Science Reviews*, 135, 17–37. <https://doi.org/10.1016/j.earscirev.2014.03.011>
- Siebel, W., Eroğlu, S., Shang, C. K., & Rohrmüller, J. (2012). Zircon geochronology, elemental and Sr-Nd isotope geochemistry of two Variscan granitoids from the Odenwald-Spessart crystalline complex (mid-German crystalline rise). *Mineralogy and Petrology*, 105(3–4), 187–200. <https://doi.org/10.1007/s00710-012-0200-3>
- Slingerland, R. L. (1977). The effects of entrainment on the hydraulic equivalence relationships of light and heavy minerals in sands. *Journal of Sedimentary Petrology*, 47(2), 753–770. <https://doi.org/10.1306/212F7243-2B24-11D7-8648000102C1865D>
- Soyk, D. (2015). *Diagenesis and reservoir quality of the lower and Middle Buntsandstein (lower Triassic), SW Germany*, (Doctoral dissertation). University Heidelberg. Retrieved from <https://archiv.ub.uni-heidelberg.de/volltextserver/18871/1/DissertationSoyk.pdf>
- Stein, E. (2001). The geology of the Odenwald crystalline complex. *Mineralogy and Petrology*, 72(1–3), 7–28. <https://doi.org/10.1007/s007100170024>
- Stein, E., Dörr, W., Helm, J., Schastok, J., & Velledits, F. (2022). Coeval subduction and collision at the end of the Variscan orogeny (Odenwald, Mid-German Crystalline Zone, Germany). *Zeitschrift der Deutschen Gesellschaft für Geowissenschaften*, 173(1), 211–236. <https://doi.org/10.1127/zdgg/2022/0287>
- Stone, M., & Saunderson, H. (1992). Particle size characteristics of suspended sediment in southern Ontario rivers tributary to the great lakes. *Hydrological Processes*, 6(2), 189–198. <https://doi.org/10.1002/hyp.3360060207>
- Stutenbecker, L., Costa, A., Bakker, M., Anghileri, D., Molnar, P., Lane, S. N., & Schlunegger, F. (2019). Disentangling human impact from natural controls of sediment dynamics in an Alpine catchment. *Earth Surface Processes and Landforms*, 44(14), 2885–2902. <https://doi.org/10.1002/esp.4716>
- Stutenbecker, L., Scheuvs, D., Hinderer, M., Hornung, J., Petschick, R., Raila, N., & Schwind, E. (2023). Granulometry, geochemistry and mineralogy of fluvial sediment from the Gersprenz, Modau, Muemling, and upper Neckar rivers, Germany [Dataset]. PANGAEA. <https://doi.org/10.1594/PANGAEA.959006>
- Tofelde, S., Bernhardt, A., Guert, L., & Romans, B. W. (2021). Times associated with source-to-sink propagation of environmental signals during landscape transience. *Frontiers in Earth Science*, 9, 628315. <https://doi.org/10.3389/feart.2021.628315>
- van der Perk, M., & Espinoza Vilches, A. (2020). Compositional dynamics of suspended sediment in the Rhine River: Sources and controls. *Journal of Soils and Sediments*, 20(3), 1754–1770. <https://doi.org/10.1007/s11368-019-02490-5>
- Van Dongen, R., Scherler, D., Wittmann, H., & von Blanckenburg, F. (2019). Cosmogenic <sup>10</sup>Be in river sediment: Where grain size matters and why. *Earth Surface Dynamics*, 7(2), 393–410. <https://doi.org/10.5194/esurf-7-393-2019>
- von Blanckenburg, F. (2005). The control mechanisms of erosion and weathering at basin scale from cosmogenic nuclides in river sediment. *Earth and Planetary Science Letters*, 237(3–4), 462–479. <https://doi.org/10.1016/j.epsl.2005.06.030>
- von Eynatten, H., Tolosana-Delgado, R., & Karius, V. (2012). Sediment generation in modern glacial settings: Grain-size and source-rock control on sediment composition. *Sedimentary Geology*, 280, 80–92. <https://doi.org/10.1016/j.sedgeo.2012.03.008>
- von Eynatten, H., Tolosana-Delgado, R., Karius, V., Bachmann, K., & Caracciolo, L. (2016). Sediment generation in humid Mediterranean setting: Grain-size and source-rock control on sediment geochemistry and mineralogy (Sila Massif, Calabria). *Sedimentary Geology*, 336, 68–80. <https://doi.org/10.1016/j.sedgeo.2015.10.008>
- Walling, D. E., & Moorehead, P. W. (1987). Spatial and temporal variation of the particle-size characteristics of fluvial suspended sediment. *Geografiska Annaler*, 69(1), 47–59. <https://doi.org/10.1080/04353676.1987.11880196>
- Walling, D. E., & Woodward, J. C. (2000). Effective particle size characteristics of fluvial suspended sediment transported by lowland British rivers. The role of erosion and sediment transport in nutrient and contaminant transfer. In *Proceedings of a symposium held at Waterloo* (Vol. 263). IAHS Publ.
- Weltje, G. J. (1997). End-member modeling of compositional data: Numerical-statistical algorithms for solving the explicit mixing problem. *Mathematical Geology*, 29(4), 503–549. <https://doi.org/10.1007/BF02775085>
- Weltje, G. J., Paredis, B., Caracciolo, L., & Heins, W. A. (2018). Quantitative analysis of crystal-interface frequencies in granitoids: Implications for modelling of parent-rock texture and its influence on the properties of plutoniclastic sands. *Sedimentary Geology*, 375, 72–85. <https://doi.org/10.1016/j.sedgeo.2018.01.004>
- Will, T. M., Lee, S.-H., Schmädicke, E., Frimmel, H. E., & Okrusch, M. (2015). Variscan terrane boundaries in the Odenwald-Spessart basement, Mid-German Crystalline Zone: New evidence from ocean ridge, intraplate and arc-derived basaltic rocks. *Lithos*, 220–223, 23–42. <https://doi.org/10.1016/j.lithos.2015.01.018>
- Will, T. M., & Schmädicke, E. (2001). A first find of retrogressed eclogites in the Odenwald crystalline complex, Mid-German crystalline rise, Germany: Evidence for a so far unrecognised high-pressure metamorphism in the Central Variscides. *Lithos*, 59(3), 109–125. [https://doi.org/10.1016/S0024-4937\(01\)00059-7](https://doi.org/10.1016/S0024-4937(01)00059-7)
- Will, T. M., & Schmädicke, E. (2003). Isobaric cooling and anti-clockwise P–T paths in the Variscan Odenwald Crystalline Complex, Germany. *Journal of Metamorphic Geology*, 21(5), 469–480. <https://doi.org/10.1046/j.1525-1314.2003.00453.x>
- Will, T. M., Schmädicke, E., Ling, X.-X., Li, X.-H., & Li, Q.-L. (2021). Geochronology, geochemistry and tectonic implications of Variscan granitic and dioritic rocks from the Odenwald-Spessart basement, Germany. *Lithos*, 404–405, 106454. <https://doi.org/10.1016/j.lithos.2021.106454>
- Xu, J. (2002). Implication of relationships among suspended sediment size, water discharge and suspended sediment concentration: The Yellow River basin, China. *Catena*, 49(4), 289–307. [https://doi.org/10.1016/S0341-8162\(02\)00064-4](https://doi.org/10.1016/S0341-8162(02)00064-4)
- Ziegler, P. A. (1992). European Cenozoic rift system. *Tectonophysics*, 208(1–3), 91–111. [https://doi.org/10.1016/0040-1951\(92\)90338-7](https://doi.org/10.1016/0040-1951(92)90338-7)